

$p(n \times 1)$ superstructures of Pb on Cu(110)

C. Nagl, M. Pinczolics, M. Schmid, and P. Varga*

Institut für Allgemeine Physik, Technische Universität Wien, A-1040 Wien, Austria

I. K. Robinson

Department of Physics, University of Illinois at Urbana-Champaign, Urbana, Illinois 61801

(Received 28 June 1995)

The structures of the $p(n \times 1)$ superstructures ($n = 4, 5,$ and 9) of Pb on Cu(110) in the coverage range between $\Theta = 0.75$ and 0.8 are revealed by atomically resolved scanning tunneling microscopy. All three superstructures are formed by substitution of every n th row of Cu atoms ($n = 4, 5,$ and 9) in the $[001]$ direction by Pb atoms. The Pb atoms in between are lined up in the $[\bar{1}10]$ direction. The $p(4 \times 1)$ structure appears in two different modifications: one with substitutional rows of Pb atoms and one with a simple overlayer structure without substituted rows of Cu atoms. Alternating succession of these two modifications results in $p(12 \times 1)$ domains. It is further shown that the $p(9 \times 1)$ structure is not a succession of $p(4 \times 1)$ and $p(5 \times 1)$ but a superstructure on its own. The $p(5 \times 1)$ structure proposed here agrees with previous x-ray-diffraction data at least as well as the quasihexagonal model proposed earlier. We have, in addition, identified the nature of the phase that has been described incommensurate obtained by desorption of Pb upon annealing above 600 K.

I. INTRODUCTION

Submonolayer Pb films on Cu(110) show a variety of superstructure phases (SP's) depending on coverage.¹⁻⁴ A surface alloy lattice gas at low coverage⁵ is followed by a $c(2 \times 2)$ SP at $\Theta = 0.5$, a $p(4 \times 1)$ at $\Theta = 0.75$, a $p(9 \times 1)$ at $\Theta = 0.778$, and a $p(5 \times 1)$ at $\Theta = 0.8$ ML Pb.³ The first detailed crystallographic study of the $p(5 \times 1)$ SP was done by Brennan, Fuoss, and Eisenberger² using grazing-incidence x-ray scattering. They described this structure as "ruffled dimers," which form zigzag chains, resulting in a quasihexagonal structure. The $p(4 \times 1)$ SP has been described in Ref. 4 as three rows of Pb atoms in a hexagonal arrangement followed by a light domain wall in the $[001]$ direction. The transition from the $p(4 \times 1)$ to the $p(5 \times 1)$ SP has therefore been explained by a "random elimination of light domains walls" resulting in a quasicompact hexagonal $p(5 \times 1)$ overlayer.⁶ A variety of SP's $\{p(n \times 1), n = 4, 17, 13, 9, 14, 19, \text{ and } 5\}$ was observed in the coverage range between $p(4 \times 1)$ and $p(5 \times 1)$, which were interpreted as a linear combination of different numbers of $p(4 \times 1)$ and $p(5 \times 1)$ SP's.⁶

In this work, we present a scanning tunneling microscopy (STM) study of the growth of Pb on Cu(110) in the coverage range between $\Theta = 0.75$ $\{=p(4 \times 1)\}$ and $\Theta = 0.8$ $\{=p(5 \times 1)\}$. Atomically resolved images allow us to present the structures of the $p(4 \times 1)$, $p(9 \times 1)$, and the $p(5 \times 1)$ SP's which are found to be substantially different from all the structures proposed in the literature.^{1,2,4}

II. EXPERIMENT

The STM work was done in an UHV chamber equipped with sample characterization equipment such as low-energy electron diffraction (LEED) and Auger elec-

tron spectroscopy (AES). The base pressure in this chamber is typically below 5×10^{-11} mbar. All STM images were obtained in constant current mode with the sample negative. Tunneling voltages and currents were between -1 V and -5 mV and 0.7 and 4 nA, respectively. The sample preparation (sputter cleaning, annealing, and Pb deposition) was performed in a separate chamber with a pressure in the low 1×10^{-10} -mbar region. The Cu(110) single crystal was cleaned by cycles of Ar^+ sputtering and annealing to 800 K. Pb (99.999%) was deposited from an electron-beam-heated crucible at deposition rates between 0.05 and 1 ML/min (a coverage of $\Theta = 1$ ML corresponds to one Pb atom per one Cu atom). The deposition rate was controlled by a quartz microbalance before the deposition and continuously monitored by the built-in flux monitor of the evaporation source (Omicron EFM3) with an accuracy estimated to be better than $\pm 5\%$. Furthermore, the coverage has been routinely controlled by AES after the STM measurements and by comparison with superstructures known from literature. With the help of these superstructures the actual coverage can be determined within 1% accuracy.

All the STM experiments and the Pb deposition were performed at room temperature (RT). When denoted in the figure captions, the sample has been annealed after Pb deposition to reduce the domain boundary and the island density, respectively.

III. RESULTS

A. $p(4 \times 1)$ superstructure

Figure 1 shows a STM image of the Cu(110) surface after RT deposition of $\Theta = 0.75$ ML Pb, the coverage necessary for the formation of the $p(4 \times 1)$ SP. Grooves are visible in the $[001]$ direction with mainly two different

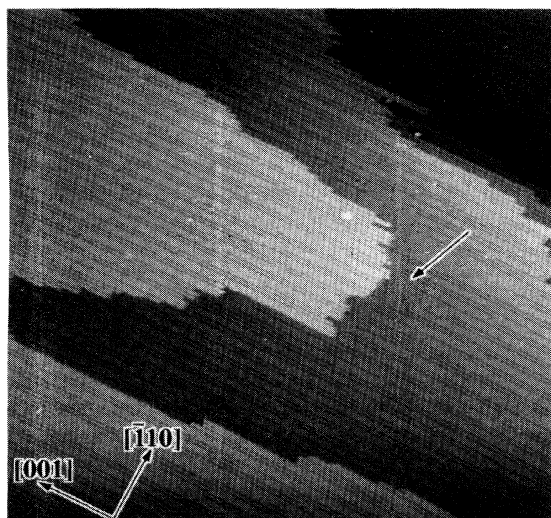


FIG. 1. STM image of $\Theta=0.75$ ML Pb deposited on Cu(110) at RT after annealing to 420 K. Almost the whole surface exhibits grooves with mainly two different spacings, which succeed each other fairly regularly. The region marked by an arrow shows no grooves ($1000 \times 1000 \text{ \AA}^2$).

spacings. These grooves are oriented perpendicular to the direction of the natural $[\bar{1}10]$ troughs seen on clean Cu(110) surfaces. Close to a step edge a small region without any groove can be seen (marked by an arrow). A detail of the above image shows an area with small groove spacings as well as larger spacings (Fig. 2). The minimum distance between two grooves spacings corre-

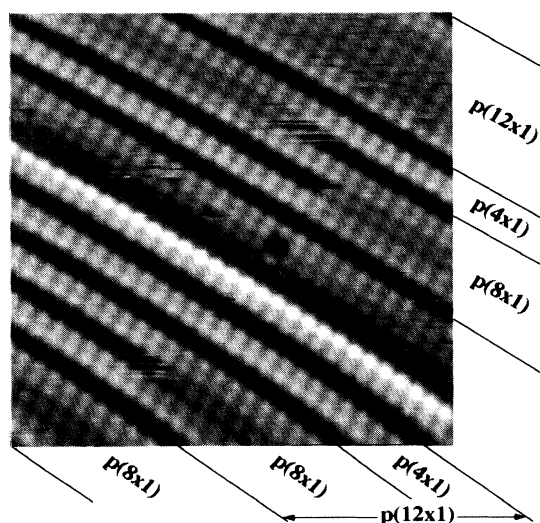


FIG. 2. STM image of $\Theta=0.75$ ML Pb. The two modifications of the $p(4 \times 1)$ superstructure result in the local formation of $p(8 \times 1)$ and $p(12 \times 1)$ superstructures. Burrowing of a row of Pb atoms leads to the transformation of a $p(8 \times 1)$ into a $p(4 \times 1)$ structure and vice versa. For better contrast, the height of the step has been reduced artificially ($100 \times 100 \text{ \AA}^2$).

sponds exactly to four Cu lattice constants, i.e., a $p(4 \times 1)$ SP. In between these two closely spaced grooves two Pb atoms are visible. The coverage (which is known with an accuracy of about 5%) of 0.75 ML Pb, however, implies that there have to be three Pb atoms placed on four Cu atoms. Therefore, the missing Pb atom has to be in the groove; i.e., the grooves are filled with Pb atoms that have replaced a row of Cu atoms and are situated in the first Cu layer. This is also confirmed by the highest coverage SP, the $p(5 \times 1)$, which has the highest groove density (see below). If the grooves were not filled with Pb a higher groove density would result in a lower coverage. Electronic and tip effects can be excluded to cause the grooves since they are independent of tunneling conditions. Furthermore, we have observed islands which appear on large terraces, i.e., the expelled Cu atoms either diffuse to steps or form islands that are again covered by the corresponding SP. Successive images show that these grooves can move or even disappear. This movement also causes the frizzy appearance of the end of the grooves in Fig. 2. The overall coverage and the movement, however, imply that the structure with the larger groove spacing as well as the one with the smaller spacing are two modifications of the $p(4 \times 1)$ SP. In other words, the $p(4 \times 1)$ SP also appears as an overlayer struc-

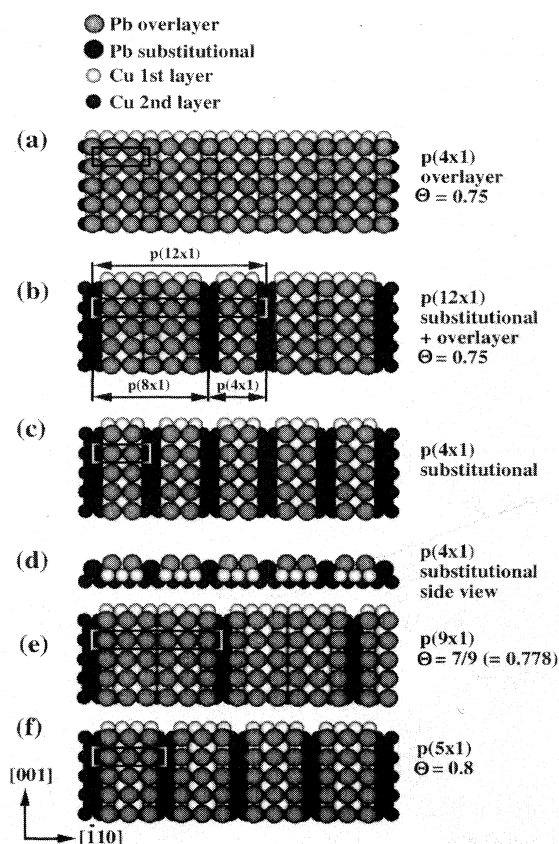


FIG. 3. Unit cells of the $p(n \times 1)$ superstructures ($n=4, 12, 9$, and 5) and the corresponding coverage. (a) and (c) show the two different modifications of the $p(4 \times 1)$ superstructure. The unit cells are marked by a rectangle.

ture without any grooves (see the region marked by an arrow in Fig. 1). The succession of these two different modifications leads to small domains of $p(8 \times 1)$ SP's and $p(12 \times 1)$ SP's, where the latter can be understood as a $p(8 \times 1)$ SP followed by a $p(4 \times 1)$ SP. Figures 3(a) and 3(c) show models of the two modifications of the $p(4 \times 1)$ SP which are different from those presented in the literature so far.^{1,4}

B. $p(9 \times 1)$ superstructure

After adding about 0.025 ML Pb (total coverage 0.775 ML), the whole surface exhibits grooves with two different spacings [Fig. 4(a)]. This is more clearly seen in a closeup shown in Fig. 5. Besides the two modifications of the $p(4 \times 1)$ SP, a different structure appears in which every *seventh* row of Pb's is situated in the underlying Cu layer, i.e., substitutes a row of Cu atoms in the [001] direction. The atoms in between are—similar to the $p(4 \times 1)$ SP—lined up in the $[\bar{1}10]$ direction. This structure cannot be explained by an alternating succession of the two modifications of the $p(4 \times 1)$ SP [i.e., a $p(8 \times 1)$ SP], since in this case every *sixth* row of Pb would be situated in the underlying Cu layer. From the distance of the grooves and the number of Pb atoms in between, it is obvious that seven Pb atoms are placed on nine Cu atoms. That is to say, this structure is a $p(9 \times 1)$ SP with a local coverage of $\frac{7}{9}$ ($=0.778$) ML Pb. Figure 3(e) shows the $p(9 \times 1)$ SP schematically. At an overall coverage of $\Theta=0.778$ ML Pb, the whole surface is covered by the $p(9 \times 1)$ SP (Fig. 6).

Figure 4(b) shows the result of an experiment where a 0.757 ML Pb film has been cooled down from 430 to 370

K in about 14 h. The experimental parameters have been chosen to account for the “very slow kinetics of the domain wall pinning transition,” as described in Ref. 3. Indeed, Fig. 4(b) shows a very regular succession of small and large groove spacings that can be related to $p(4 \times 1)$ and $p(8 \times 1)$ or $p(9 \times 1)$ SP's. That is to say, the alternation of unit cells from each of simple SP's leads to the formation of $p(12 \times 1)$ and $p(13 \times 1)$ SP's, respectively.

C. $p(5 \times 1)$ superstructure

After further increase of the coverage, a structure appears with a smaller groove-to-groove distance than the $p(9 \times 1)$ SP [Fig. 7(a)]. A detail of Fig. 7(a) shows that this structure is formed by three rows of Pb atoms in the overlayer, again followed by a substitutional row of Pb atoms [Fig. 7(b)]. Since in this case four Pb atoms are situated on five Cu atoms, this structure has to be a $p(5 \times 1)$ SP with a local coverage of $\Theta=0.8$ ML Pb [a schematic drawing is presented in Fig. 3(f)].

Further deposition of Pb above $\Theta=0.8$ ML Pb leads to the formation of three-dimensional (3D) islands on top of the Pb overlayer,¹ consistent with this being the structure at saturation coverage, although locally a $p(6 \times 1)$ SP with $\Theta=0.833$ [Fig. 7(b)] and even a $p(2 \times 1)$ with $\Theta=1$ could be observed [Fig. 7(c)].

The depth of the grooves measured with STM is between 0.6 and 0.8 Å, which is in reasonable correspondence with the rough estimation of a hard-sphere model (see Fig. 8). In this model, the depth is about 1.25 Å. Due to this large depth, we could not succeed in imaging the Pb atoms that are situated in the grooves.

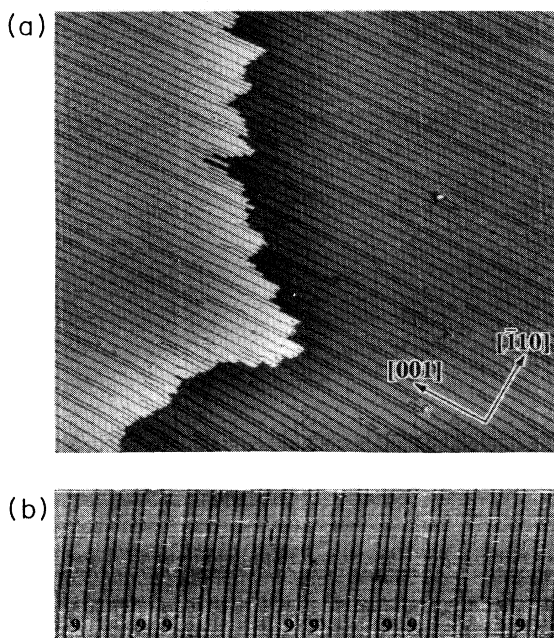


FIG. 4. (a) STM image of $\Theta=0.775$ ML Pb on Cu(110) deposited at RT and annealed at 470 K. Visible is a more or less regular arrangement of $p(4 \times 1)$ and $p(9 \times 1)$ superstructures, with small and large groove to groove spacings, respectively ($1000 \times 1000 \text{ \AA}^2$). (b) STM image of $\Theta=0.76$ ML Pb after cooling down from 430 to 370 K in 14 h. The $p(9 \times 1)$ superstructure domains are marked by “9’s,” and all others are $p(4 \times 1)$ and $p(8 \times 1)$ structures, respectively ($1000 \times 200 \text{ \AA}^2$).

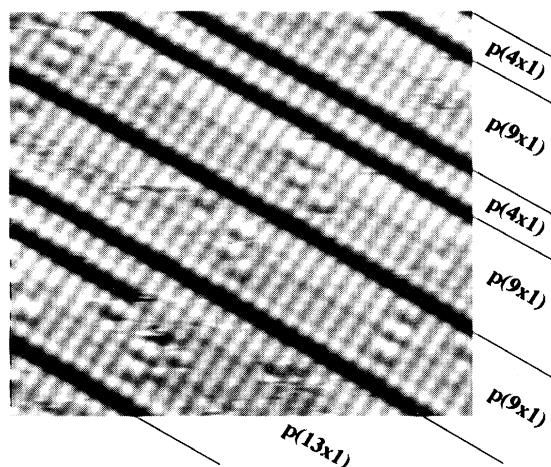


FIG. 5. STM image of $\Theta=0.775$ ML Pb. $p(4 \times 1)$, $p(9 \times 1)$, and one small domain of a $p(13 \times 1)$ superstructure are visible ($100 \times 100 \text{ \AA}^2$).

IV. DISCUSSION

A. $p(n \times 1)$ superstructures

The atomically resolved images of the $p(4 \times 1)$, $p(9 \times 1)$, and $p(5 \times 1)$ SP's shown in Figs. 2, 6, and 7(b), respectively, clearly disprove the models presented so far in the literature.^{1,2,4} Only overlayer structures had been considered by these authors, whereas our findings show substitutional structures instead. In detail, the $p(5 \times 1)$ SP has been described as a pseudo-hexagonal overlayer,^{2,4} and the $p(4 \times 1)$ SP as domains of a $p(5 \times 1)$ SP separated by light domain walls in the $[001]$ direction after every third row of Pb atoms.⁴ The $p(9 \times 1)$ SP has been described as an alternating succession of $p(4 \times 1)$ and

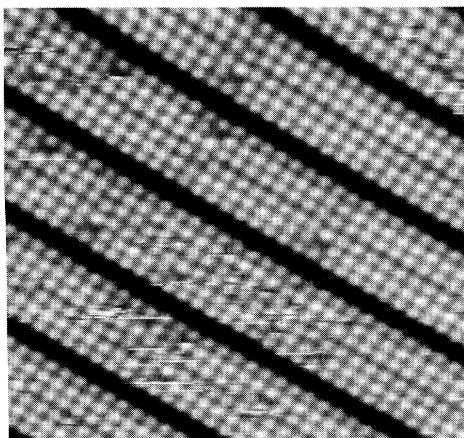


FIG. 6. STM image of a $p(9 \times 1)$ superstructure at a coverage of $\Theta=0.778$ ML Pb. Every ninth row of Cu atoms in the $[001]$ direction is replaced by a row of Pb atoms situated in the dark groove ($100 \times 100 \text{ \AA}^2$).

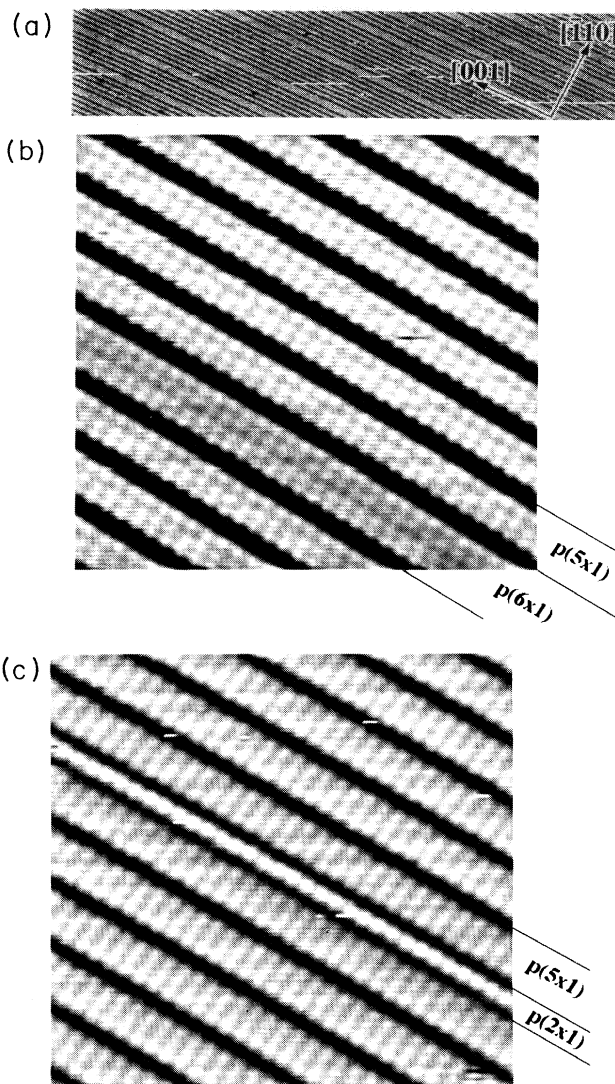


FIG. 7. (a) STM image of $\Theta=0.794$ ML Pb on Cu(110). Visible are smaller and larger groove spacings of $p(5 \times 1)$ and $p(9 \times 1)$ superstructures, respectively ($1000 \times 200 \text{ \AA}^2$). STM image of the $p(5 \times 1)$ superstructure with one domain of (b) a $p(2 \times 1)$ superstructure which has a local coverage of $\Theta=0.83$ ML Pb and (c) a $p(2 \times 1)$ superstructure which has a local coverage of $\Theta=1$ ($100 \times 100 \text{ \AA}^2$).

$p(5 \times 1)$ unit cells.⁴ However, our measurements show that the $p(n \times 1)$ SP's ($n=4, 9$, and 5) are formed by substitution of every n th row of Cu atoms by Pb atoms.

In an earlier x-ray study,² the formation of an incommensurate phase, with a floating hexagonal layer structure which forms upon annealing of the $p(5 \times 1)$ SP at 623 K, has been reported. Contrary to these findings, we observe that heating of the $p(5 \times 1)$ SP leads to desorption of Pb, starting at around 570 K, and the succession of phases is entered in the inverse order to that seen upon deposition. No floating hexagonal phase was ever observed. A better description of the incommensurate state would therefore be called discommensurate, as it is made up of a random sequence of unit cells of different simple

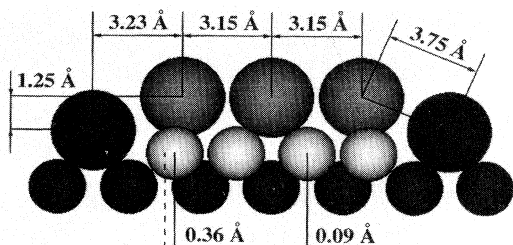


FIG. 8. Model for the $p(5 \times 1)$ superstructure. The in-plane distances have been derived by recalculation of the x-ray-diffraction data in Ref. 2; the height difference of 1.25 Å between the overlayer Pb atoms and the Pb atoms in the groove is a rough estimation resulting from a hard-sphere model.

SP structures, for example $p(5 \times 1)$ and $p(9 \times 1)$. The diffraction from a 1D structure made up of a random sequence of two different lengths was derived by Hendricks and Teller,⁷ and yields a single broadened diffraction peak in between the positions of the two parent phases. Just such a broadened peak was indeed observed by Brennan, Fuoss, and Eisenberger in Ref. 2.

A recent x-ray study of the $p(4 \times 1)$ SP of Bi on Cu(110) (Ref. 8) showed the same substitutional structure as has been described within this work. Since beside this $p(4 \times 1)$ SP, $p(n \times 1)$ SP's also have been found in other deposition studies on Bi on Cu(110) ($n=4, 5,$ and 6) (Ref. 9) and of Pb on Ni(110) ($n=3, 4,$ and 5),¹⁰ we suggest these SP's may likewise be of the substitutional type.

On closer look, another interesting result can be deduced from Fig. 2: even though the row of Pb atoms that is in the middle of the two $p(8 \times 1)$ domains in the lower part of the image is situated in bridge sites [see the model in Fig. 3(a)], it appears darker. This unexpected behavior, which has also been observed on a close-packed Pb film on Cu(111), will be the subject of a future publication.¹¹

B. Reconciliation with previous x-ray-diffraction study

A quasihexagonal Pb-overlayer structure was proposed for the $p(5 \times 1)$ phase in Ref. 2, which gave excellent agreement with the 18 in-plane structure factor measurements. The model proposed is unusual in that it contains distortions from ideal hexagonal packing which do not uphold the pmm symmetry of the Cu(110) substrate. This was permitted in the analysis of that study² because the data were not symmetry averaged, and because small differences between pmm -symmetry-related reflections were indeed observed. If these differences were truly significant (and not due to experimental error), they might be caused by a low symmetry overlayer (such as the one proposed in Ref. 2) with a preferred orientation among the inequivalent domains, that might be caused by miscut of the sample used, for example.

In none of our STM images have we detected evidence of the broken pmm symmetry of the $p(5 \times 1)$ phase; nor have we seen unit cells with hexagonal packing apparent in the topmost layer. In an attempt to resolve this rather serious discrepancy, we consider an alternative explana-

tion of the observed broken symmetry; that it simply represents the experimental uncertainty of the structure factor measurements. Tiny misalignments or deviations of the grazing incidence angle from the critical angle can lead to systematic errors of the magnitude of the observed variation.

The x-ray study² was one of the earliest of its kind, and numerous subsequent analyses have assumed instead that the nonreproducibility of symmetry-equivalent reflections is due to systematic errors.¹² In fact, the determination of the reproducibility has become the accepted way to determine experimental errors in surface x-ray crystallography,^{13,14} just as it is indeed used in traditional x-ray crystallography.¹⁵

A second difference in the x-ray analysis of Ref. 2 was the omission of structure-factor contributions from the Cu bulk crystal. It is now known that an ideal 1×1 bulk-terminated surface of a fcc(110) crystal will have surface diffraction at in-plane positions, where the crystal truncation rods (CTR's) (Ref. 16) intersect the plane. These contributions are important only for integer-order reflections, of which there are two in the published data set, one identically zero and the other rather small. Knowing now that there must be a CTR contribution from the Cu substrate, we must conclude that there must be a cancellation from the structure-factor amplitude of the Pb overlayer present.

We therefore reanalyzed the data from Ref. 2 following the now-conventional analysis procedure.^{13,14} We took the 18 corrected intensity values and performed the averaging over the pmm symmetry. The average of their discrepancy (18%) was then taken to be the systematic error of the data; the random error was estimated very roughly to be half the weakest measured nonzero intensity value. These errors were combined in quadrature to give an overall error estimate. We then fit calculated structure factors for various 2D projected models to the square root of the previously measured intensities, weighted by the reciprocal of the estimated errors.

The calculated intensities quoted in Ref. 2 indeed correspond to a very good agreement with a statistical χ^2 value of 0.8, but this corresponds to a calculation for a single domain with broken pmm symmetry, and no CTR contributions. If we attempt to fit the same model constrained by symmetry with the CTR contributions, we obtain $\chi^2=2.29$ instead. Relaxing the symmetry, but assuming equal contributions from the mirror-related domains, leads to $\chi^2=1.71$.

The model for the $p(5 \times 1)$ phase in Fig. 3(f), as derived from STM measurements, was tested as well. Assuming pmm symmetry, the model has three free displacement parameters, all along the long axis of the unit cell. Allowing these parameters and one scale factor to vary, we obtained a good fit with $\chi^2=1.67$. If our error estimate above is correct, this means the fit is close to perfect at the level of the available data, and that little further information can be expected. The refined positions of the atoms are shown in Fig. 8, and the resulting agreement with the experimental data in Fig. 9. The important conclusion is that the model fits the experimental data of Ref. 2 at least as well as the model of Ref. 2, once the

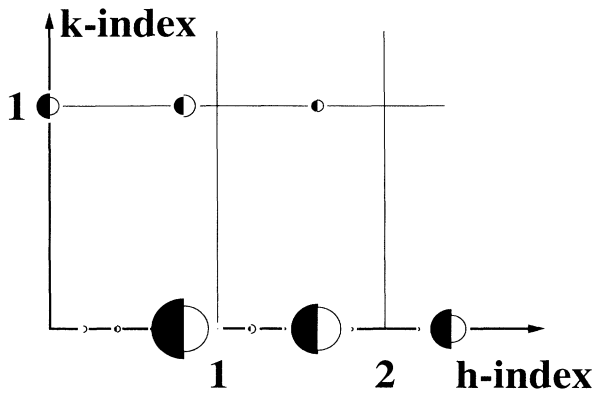


FIG. 9. Comparison of observed x-ray structure factors for the $p(5 \times 1)$ phase of Pb/Cu(110) (Ref. 2) and those calculated for the model proposed in this paper. The radius of each semicircle is proportional to the structure factor amplitude; the area is proportional to its intensity. The observed values are shaded, the calculated ones open. This least-squares fit gave a statistical χ^2 of 1.67.

symmetry and CTR contributions are included.

We can use the x-ray analysis as further proof of the existence of alloying of Pb and Cu in the second layer of the model. The chemical identity of the atoms is not well defined by STM, and we used the coverage data to identify the phases above. The contrast between Pb and Cu is excellent with x-ray diffraction, on the other hand. We tested the effect of replacing the second-layer Pb atom in the model of Fig. 3(f) with another Cu, and repeated the refinement. We obtained a χ^2 of 5.6, effectively ruling out this possibility.

The three positional parameters used in the fitting are displayed in Fig. 8. The top-layer Pb-Pb distance of 3.15 Å is $11 \pm 3\%$, contracted from bulk Pb; this is reasonable considering its low coordination number. In the second layer, we find a lateral Pb-Cu distance of 2.91 Å, or $4 \pm 3\%$ contracted from the average spacing of bulk Pb and bulk Cu; this is reasonable since these atoms are close to fully coordinated. More surprising are the Cu-Cu separations of 2.10 ± 0.13 and 2.73 ± 0.16 Å, representing a 20% contraction and a 7% expansion. This is partly understood to be caused by accommodation of the Pb overlayer: the central Pb can drop down into its symmetric (4-coordinated) site, pushing apart and overlapping with the Cu, while the off-center Cu's do not pack so well and cause the Cu's to bond more strongly to each other. As indicated, the error bars in the determination are rather large and do not permit a more detailed analysis.

C. Energy and stress considerations

The substitution of Cu surface atoms by Pb atoms seems to be a common phenomenon despite the bulk immiscibility. Surface alloy formation in the low-coverage regime has been observed on all three low-index surfaces [for Cu(111), see Ref. 17; for Cu(110), see Ref. 5; and for Cu(100), see Ref. 13; for other systems where surface alloying has also been observed, see, e.g., Ref. 18 and references therein]. Furthermore, on Cu(100) an ordered

$c(4 \times 4)$ surface alloy structure was observed.^{19,20} Also, in our case the formation of substitutional SP's is favorable to the pseudohexagonal overlayer proposed in Refs. 2 and 4.

In terms of coordination, for each substitutional Pb atom the groove structure has four Pb-Cu bonds more and two Cu-Cu and two Pb-Pb bonds fewer than an overlayer chain structure such as the second modification of the $p(4 \times 1)$. We expect the strength of a Pb-Cu bond to be between that of Cu-Cu and Pb-Pb, which would indicate that the energy associated with the formation of the grooves is rather small. This is related to the fact that the groove structure avoids the Pb sites with the lowest coordination in the overlayer chain structure, i.e., those in bridge sites.

The long-range order found, e.g., in Figs. 1 and 4(b) [$p(12 \times 1)$ and $p(13 \times 1)$ superstructures] cannot be explained by the groove energy but rather are indicative of a stress effect. Relief of compressive stress at high Pb coverages may also explain why the corresponding SP's always exhibit grooves, whereas the $p(4 \times 1)$ occurs in two modifications.

V. CONCLUSION

By means of atomically resolved STM images, the structures of the $p(n \times 1)$ SP's ($n=4, 9,$ and 5) were revealed. All three SP's were found to be different from those proposed in the literature. We have shown that these structures are formed by substitution of every n th row of Cu atoms in the [001] direction ($n=4, 9,$ and 5 , corresponding to the SP unit cell) by Pb atoms. Between these rows of Pb atoms that are situated in the underlying Cu layer, the Pb atoms are lined up in the $[\bar{1}10]$ direction on the underlying Cu layer. For the $p(9 \times 1)$ and $p(5 \times 1)$ SP's, this substitution reduces the compressive stress. The least densely packed of these three structures, the $p(4 \times 1)$ SP, appears in two different modifications, transformable into each other: besides the substitutional structure there also exists a simple overlayer structure. A recalculation of the x-ray-diffraction data for the $p(5 \times 1)$ SP of Ref. 2 with the model derived by STM resulted in a better fit, and allowed us to determine the displacements of the Pb atoms in the unit cell and of the underlying Cu atoms, respectively. Annealing of the $p(5 \times 1)$ SP to 600 K led to desorption of Pb. In this way, the succession of SP's is run through in the reverse way. In other words, no evidence was found for the formation of an incommensurate SP after annealing as reported in the literature.²

ACKNOWLEDGMENTS

Helpful discussions with P. Fratzl from the Institut für Festkörperphysik, University of Vienna, concerning the recalculation and interpretation of the x-ray-diffraction data from Ref. 2 are gratefully acknowledged. This work has been supported by the "Fonds zur Förderung der wissenschaftlichen Forschung" under Project No. P9282, and by the "Hochschuljubiläumsstiftung der Stadt Wien." Work at the University of Illinois was supported by the U.S. Department of Energy under Contract No. DEFG02-91ER45439.

- *Author to whom correspondence should be addressed. FAX: +43-1-586 4203. Electronic address: varga@eps1.tuwien.ac.at
- ¹J. Henrion and G. E. Rhead, *Surf. Sci.* **29**, 20 (1972); A. Sepulveda and G. E. Rhead, *ibid.* **66**, 436 (1977).
- ²W. C. Marra, P. H. Fuoss, and P. E. Eisenberger, *Phys. Rev. Lett.* **49**, 1169 (1982); S. Brennan, P. H. Fuoss, and P. Eisenberger, *Phys. Rev. B* **33**, 3678 (1986).
- ³C. H. Lee, E. Y. Sheu, K. S. Liang, K. L. D'Amico, and W. N. Unertl, *Appl. Phys. A* **51**, 191 (1990); K. S. Liang, K. L. D'Amico, C. H. Lee, and E. Y. Sheu, *Phys. Rev. Lett.* **65**, 3025 (1990).
- ⁴C. de Beauvais, D. Rouxel, B. Bigeard, and B. Mutaftschiev, *Phys. Rev. B* **44**, 4024 (1991).
- ⁵C. de Beauvais, D. Rouxel, Michail Michailov, and B. Mutaftschiev, *Surf. Sci.* **324**, 1 (1995).
- ⁶C. de Beauvais, D. Rouxel, B. Mutaftschiev, and B. Bigeard, *Surf. Sci.* **272**, 73 (1992).
- ⁷S. B. Hendricks and E. Teller, *J. Phys. Chem.* **10**, 147 (1942).
- ⁸L. Lottermoser, R. L. Johnson, T. Buslaps, R. Feidenhans'l, and M. Nielsen (private communication).
- ⁹W. D. Clendening and C. T. Campbell, *J. Chem. Phys.* **90**, 6656 (1989).
- ¹⁰J. Perereau and I. Szymerska, *Surf. Sci.* **32**, 247 (1972).
- ¹¹C. Nagl, M. Schmid, and P. Varga (unpublished).
- ¹²I. K. Robinson and D. J. Tweet, *Rep. Prog. Phys.* **55**, 599 (1992).
- ¹³I. K. Robinson, in *Handbook on Synchrotron Radiation*, edited by D. E. Moncton and G. S. Brown (Elsevier, Amsterdam, 1990), Vol. III.
- ¹⁴R. Feidenhans'l, *Surf. Sci. Rep.* **10**, 105 (1989).
- ¹⁵H. Lipson and W. Cochran, *The Determination of Crystal Structures* (Cornell University Press, Ithaca, NY, 1966).
- ¹⁶I. K. Robinson, *Phys. Rev. B* **33**, 3830 (1986).
- ¹⁷C. Nagl, O. Haller, E. Platzgummer, M. Schmid, and P. Varga, *Surf. Sci.* **321**, 237 (1994).
- ¹⁸J. Tersoff, *Phys. Rev. Lett.* **74**, 434 (1995).
- ¹⁹C. Nagl, E. Platzgummer, O. Haller, M. Schmid, and P. Varga, *Surf. Sci.* **331-333**, 831 (1995).
- ²⁰Y. Gauthier, W. Höslér, and W. Moritz, *Surf. Sci.* (to be published).

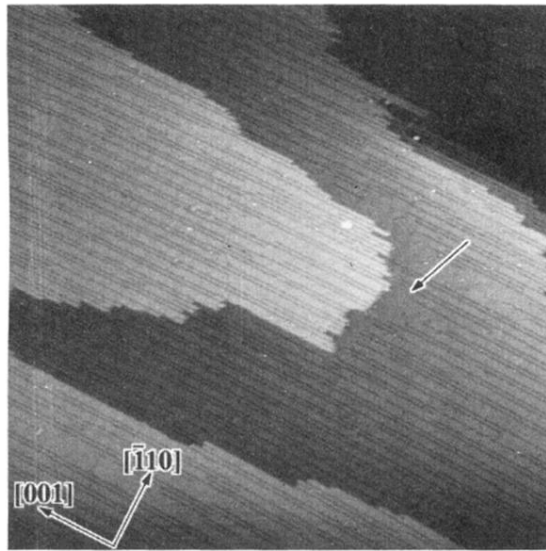


FIG 1. STM image of $\Theta=0.75$ ML Pb deposited on Cu(110) at RT after annealing to 420 K. Almost the whole surface exhibits grooves with mainly two different spacings, which succeed each other fairly regularly. The region marked by an arrow shows no grooves ($1000 \times 1000 \text{ \AA}^2$).

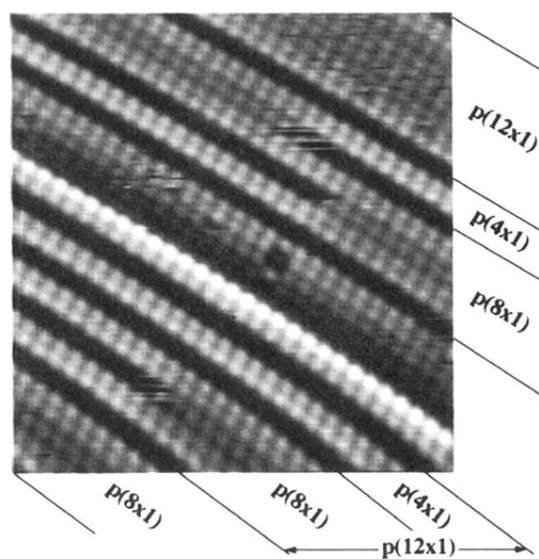


FIG. 2. STM image of $\Theta=0.75$ ML Pb. The two modifications of the $p(4 \times 1)$ superstructure result in the local formation of $p(8 \times 1)$ and $p(12 \times 1)$ superstructures. Burrowing of a row of Pb atoms leads to the transformation of a $p(8 \times 1)$ into a $p(4 \times 1)$ structure and vice versa. For better contrast, the height of the step has been reduced artificially ($100 \times 100 \text{ \AA}^2$).

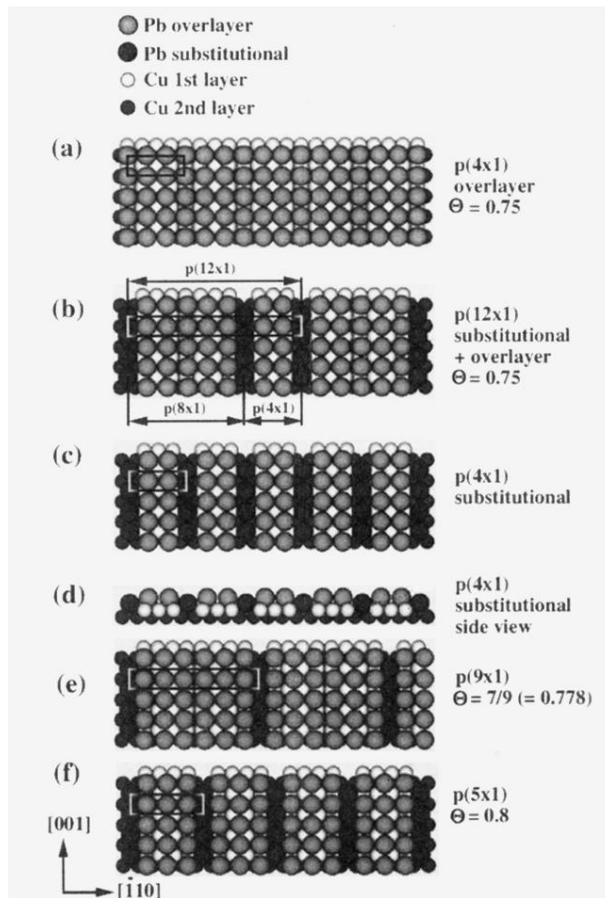


FIG. 3. Unit cells of the $p(n \times 1)$ superstructures ($n = 4, 12, 9,$ and 5) and the corresponding coverage. (a) and (c) show the two different modifications of the $p(4 \times 1)$ superstructure. The unit cells are marked by a rectangle.

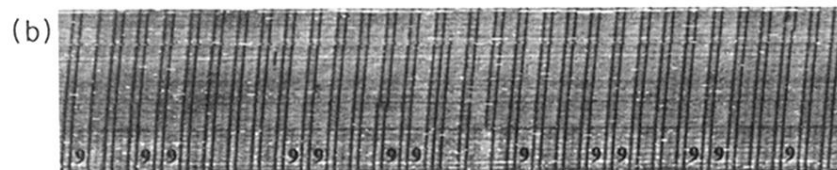
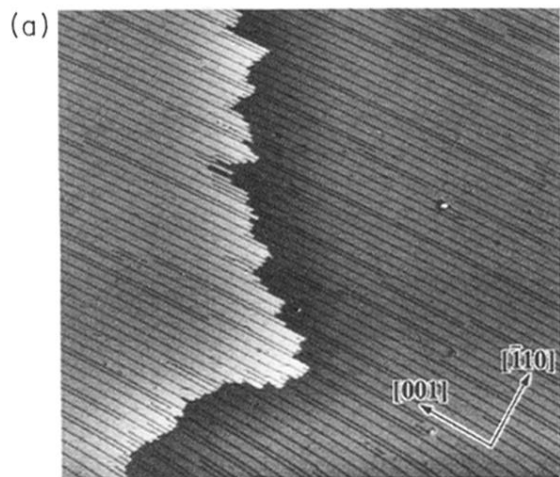


FIG. 4. (a) STM image of $\Theta=0.775$ ML Pb on Cu(110) deposited at RT and annealed at 470 K. Visible is a more or less regular arrangement of $p(4\times 1)$ and $p(9\times 1)$ superstructures, with small and large groove to groove spacings, respectively ($1000\times 1000 \text{ \AA}$). (b) STM image of $\Theta=0.76$ ML Pb after cooling down from 430 to 370 K in 14 h. The $p(9\times 1)$ superstructure domains are marked by "9's," and all others are $p(4\times 1)$ and $p_2(8\times 1)$ structures, respectively ($1000\times 200 \text{ \AA}$).

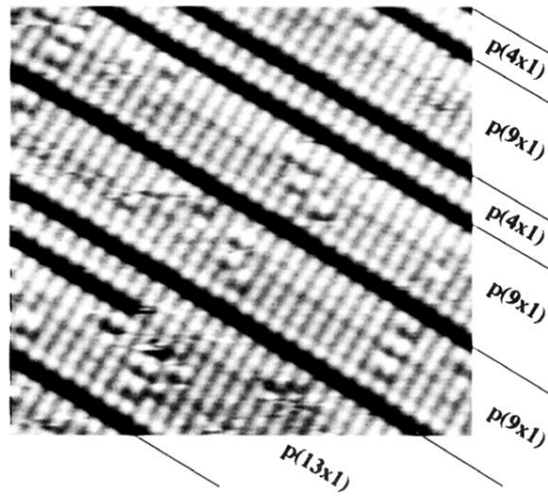


FIG. 5. STM image of $\Theta=0.775$ ML Pb. $p(4 \times 1)$, $p(9 \times 1)$, and one small domain of a $p(13 \times 1)$ superstructure are visible ($100 \times 100 \text{ \AA}^2$).

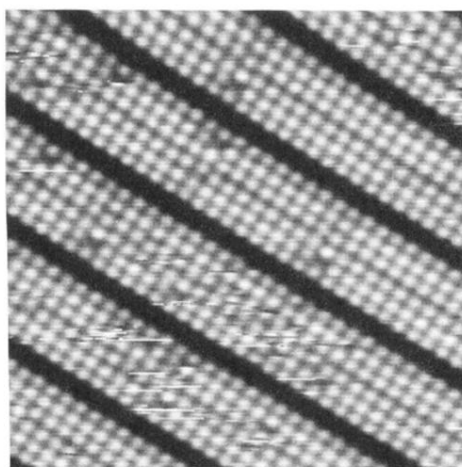


FIG. 6. STM image of a $p(9 \times 1)$ superstructure at a coverage of $\Theta = 0.778$ ML Pb. Every ninth row of Cu atoms in the [001] direction is replaced by a row of Pb atoms situated in the dark groove ($100 \times 100 \text{ \AA}^2$).

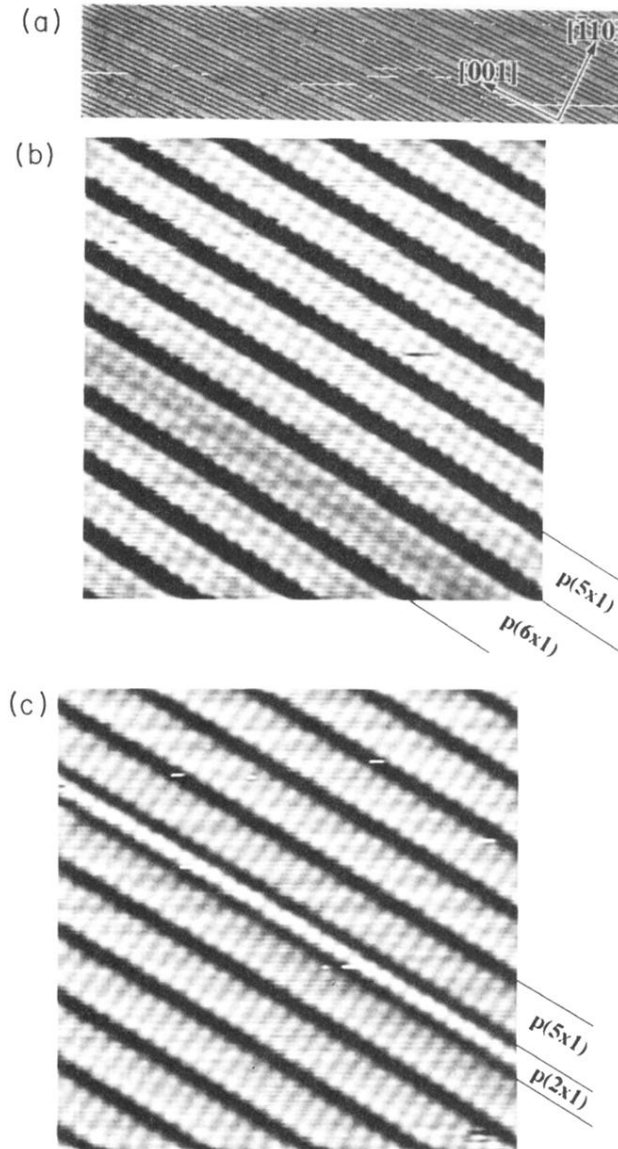


FIG. 7. (a) STM image of $\Theta=0.794$ ML Pb on Cu(110). Visible are smaller and larger groove spacings of $p(5 \times 1)$ and $p(9 \times 1)$ superstructures, respectively ($1000 \times 200 \text{ \AA}^2$). STM image of the $p(5 \times 1)$ superstructure with one domain of (b) a $p(2 \times 1)$ superstructure which has a local coverage of $\Theta=0.83$ ML Pb and (c) a $p(2 \times 1)$ superstructure which has a local coverage of $\Theta=1$ ($100 \times 100 \text{ \AA}^2$).

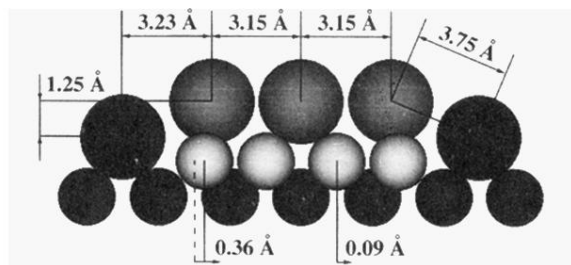


FIG. 8. Model for the $p(5 \times 1)$ superstructure. The in-plane distances have been derived by recalculation of the x-ray-diffraction data in Ref. 2; the height difference of 1.25 \AA between the overlayer Pb atoms and the Pb atoms in the groove is a rough estimation resulting from a hard-sphere model.